KSME Journal, Vol. 8, No. 2, pp. 183~190, 1994

Stress Distribution and Yield Surface Determination for Center Cracked Layered Material

Sungho Kim* and Namho Kim*

(*Received December 1, 1993*)

KSME Journal of Separate Volume

KSME Journal, Vol. 8, No. 2, pp. 183~190, 1994

Stress Distribution and Yield Surface Determination for Center Cracked Layered Material

Sungho Kim* and Namho Kim*

(Received December 1, 1993)

A model is constructed to analyze the stress and to determine the yield surface for cracked layer which is perfectly bonded to the substrate. It is assumed that the layer and substrate are isotropic and crack surface is subjected to a constant pressure. Mixed boundary value problem is formulated by Fourier integral transform method, and governing equations are reduced to a Fredholm integral equation. From the numerical analysis, stress components including Mises stress are evaluated. Finally, using the Mises yield criterion, the yield surface is determined for various layer-substrate combinations.

Key Words: Yield Surface, Layered Material, Center Crack

1. Introduction

One of important reasons for using layered materials is to improve the range of load tolerance. These layered materials may have defects and some load endurance degradations are expected. It is, therefore, of great practical importance to develop a rational and preferably simple method to evaluate the stress field for cracked layered materials. Sneddon(Sneddon, 1946) studied the stress distribution in the neighbourhood of a crack in an elastic solid. Later, Hilton and Sih(Hilton and Sih, 1970, 1971) considered the plane extension of a crack parallel to the interface. Recently, Kim and Oh(Kim et al., 1991 ; Oh et al., 1992) extended their models by introducing additional layer between cracked layer and half space, and evaluated stress intensity factors under uniaxial loading, in-plane and anti-plane loading, respectively. However, the above mentioned models concentrated only on determining the stress intensity factors.

In this analysis, Hilton and Sih's model is repeated to thoroughly evaluate stress components in the layer and the substrate including Mises stress thereby analyzing the effect of layer thickness and shear modulus ratio between the layer and the substrate.

* Agency for Defense Development, Yusung P.O. Box 35(1-2-4), Taejeon, Korea

2. Equations and Derivations

Consider a cracked elastic layer sandwiched between two substrates. The coordinate system and the geometry are shown in Fig. 1. It is assumed that the layer is perfectly bonded to the substrate. Using the Fourier integral transformation method, mixed boundary value problem in the plane theory of elasticity is formulated as follows(Sneddon,1951),

$$\sigma_{xx(j)}=\frac{1}{2\pi}\int_{-\infty}^{\infty}\frac{\partial^2 G_j}{\partial y^2}e^{-i\xi x}d\xi \tag{1}$$

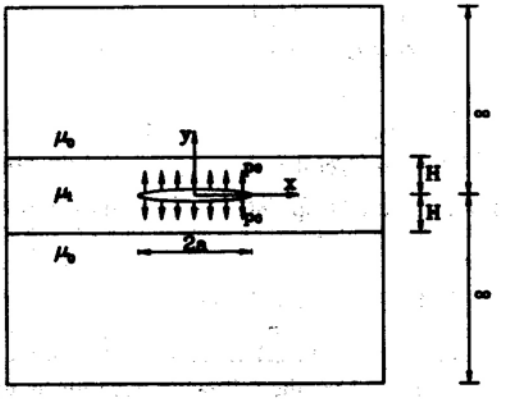

Fig. 1 Geometry and configuration of the problem

$$\sigma_{yy(j)}=\frac{-1}{2\pi}\int_{-\infty}^{\infty}\xi^2 G_j e^{-i\xi x}d\xi \tag{2}$$

$$\sigma_{xy(j)}=\frac{i}{2\pi}\int_{-\infty}^{\infty}\xi\frac{\partial G_j}{\partial y}e^{-i\xi x}d\xi \tag{3}$$

$$u_{(j)}=\frac{i}{\pi\mu_j}\int_{-\infty}^{\infty}[(1-\nu_j)\frac{\partial^2 G_j}{\partial y^2}+\nu_j\xi^2 G_j]e^{-i\xi x}d\xi/\xi \tag{4}$$

$$v_{(j)}=\frac{1}{\pi\mu_j}\int_{-\infty}^{\infty}[(1-\nu_j)\frac{\partial^3 G_j}{\partial y^3}+(\nu_j-2)\xi^2\frac{\partial G_j}{\partial y}]e^{-i\xi x}d\xi/\xi^2 \tag{5}$$

where,

$$G_1=[A_1(\xi)+\xi yB_1(\xi)]\cosh(\xi y)+[C_1(\xi)+\xi yD_1(\xi)]\sinh(\xi y) \tag{6a}$$

$$G_0=[A_0(\xi)+\xi yB_0(\xi)]e^{-\xi y} \tag{6b}$$

where, μ_j is the shear modulus, ν_j is the Poisson's ratio with subscript indices $j=0$ and 1 representing the substrate and layer, respectively. The coefficents $A_1(\xi)$, $B_1(\xi)$, $C_1(\xi)$, $D_1(\xi)$, $A_0(\xi)$ and $B_0(\xi)$ are to be determined.

2.1 Boundary conditions

When a plane strain type constant pressure is applied at the crack surface as studied by Hilton and Sih(Hilton and Sih, 1971), considerations of the upper half plane are necessary due to the geometrical symmetry. The boundary conditions are as follows,

$$\sigma_{yy(1)}=-p_0 \quad y=0 \quad -a\le x\le a \tag{7a}$$

$$v_{(1)}=0 \quad y=0 \quad x>a \text{ or } x<-a \tag{7b}$$

$$\sigma_{xy(1)}=0 \quad y=0 \quad -\infty<x<\infty \tag{8}$$

$$\sigma_{xy(1)}=\sigma_{xy(0)} \quad y=H \quad -\infty<x<\infty \tag{9}$$

$$\sigma_{yy(1)}=\sigma_{yy(0)} \quad y=H \quad -\infty<x<\infty \tag{10}$$

$$u_{(1)}=u_{(0)} \quad y=H \quad -\infty<x<\infty \tag{11}$$

$$v_{(1)}=v_{(0)} \quad y=H \quad -\infty<x<\infty \tag{12}$$

2.2 Fredholm integral equation

By applying the boundary conditions to the elasticity equations, following pair of dual integral equations are obtained.

$$\int_{-\infty}^{\infty}M(\xi)\cos\xi x d\xi=0 \qquad |x|>a \tag{13a}$$

$$\int_{-\infty}^{\infty}F(\xi)M(\xi)\cos\xi x d\xi=\pi p_0 \quad |x|\le a \tag{13b}$$

Here, $F(\xi)$ is defined as

$$\begin{bmatrix}F(\alpha)\\ d_1(\alpha)\\ a_0(\alpha)\\ b_0(\alpha)\end{bmatrix}=\vec{Q}\begin{bmatrix}\tanh z-z\\ -z\tanh z\\ -z-(1-2\nu_1)\tanh z\\ z\tanh z-2(1-\nu_1)\end{bmatrix} \tag{14a}$$

where,

$$\vec{Q}\begin{bmatrix}1 & z\tanh z & -R & -zR\\ \tanh z & z+\tanh z & R & -(1-z)R\\ 1 & 2(1-\nu_1)+z\tanh z & -\Gamma R & [2(1-\nu_2)-z]\Gamma R\\ -\tanh z & (1-2\nu_1)\tanh z-z & -\Gamma & -[(1-2\nu_1)+z]\Gamma R\end{bmatrix} \tag{14b}$$

$$\begin{bmatrix}A_1(\xi)\\ B_1(\xi)\\ C_1(\xi)\\ D_1(\xi)\\ A_0(\xi)\\ B_0(\xi)\end{bmatrix}=\begin{bmatrix}F(\alpha)\\ 1\\ -1\\ d_1(\alpha)\\ a_0(\alpha)\\ b_0(\alpha)\end{bmatrix}\frac{M(\alpha)}{\alpha} \tag{14c}$$

where,

$$\Gamma=\mu_1/\mu_0,\ z=\alpha(H/a),\quad R=e^{-z}/\cosh z,\ \xi=\alpha/a \tag{14d}$$

The method of Copson(Copson, 1961) is utilized as,

$$M(\xi)=\int_0^a\phi(t)J_0(\xi t)dt \tag{15}$$

where, $J_0(\xi t)$ is Bessel function of first kind of order zero. Then, the following equation is derived.

$$\phi(s)+\int_0^a\phi(t)K(t,s)dt=\pi p_0 s \tag{16}$$

Using the following non-dimensional parameters,

$$t=a\tau \quad s=a\sigma \quad x=a\bar{x} \quad y=a\bar{y} \tag{17a}$$

$$\phi(s)=\pi a\sqrt{\sigma}p_0\Phi(\sigma) \tag{17b}$$

Equation (16) is reduced to a Fredholm integral equation of a second kind.

$$\Phi(\sigma)+\int_0^1\Phi(\tau)K(\tau,\sigma)d\tau=\sqrt{\sigma} \tag{18a}$$

where,

$$K(\tau,\sigma)=\sqrt{\tau\sigma}\int_0^\infty\alpha[F(\alpha)-1]J_0(\alpha\tau)J_0(\alpha\sigma)d\alpha \tag{18b}$$

To solve the Fredholm integral equation, Simpson's integration technique is utilized as (Abramowitz and Stegun, 1970),

$$\Phi(\sigma_n)+\sum_{m=1}^{N_F}\Phi(\tau_m)K(\tau_m,\ \sigma_n)W(\tau_m)=\sqrt{\sigma_n}\quad(n=1,\ N_F)\tag{18c}$$

where,

$$K(\tau_m,\ \sigma_n)=\sqrt{\tau_m\sigma_n}\sum_{m=1}^{N_F}\alpha_h[F(\alpha_h)-1]J_0(\alpha_h\tau_m)J_0(\alpha_h\sigma_n)W(\alpha_h)\tag{18d}$$

Here,

τ_m, α_h : integration point
σ_m : collocation point
$W(\alpha_h)$, $W(\tau_m)$: Simpson's weight factor
N_F, N_h : number of integration point

By introducing $\tau_m=\sigma_m(m=1,\ N_F)$, Eq. (18a) becomes

$$\sum_{m=1}^{N_F}[\delta_{mn}+K(\tau_m,\ \tau_n)]\Phi(\tau_m)=\sqrt{\tau_n}\quad(n=1,\ N_F)\tag{19}$$

and finally $\Phi(\tau_m)$ can be determined numerically.

2.3 Stress distributions

At once $\Phi(\tau_m)$ is numerically determined, the stress distributions for the layer and substrate can be evaluated from Eqs. (1)~(5) and Eqs. (13)~(15) as follows,

$$\begin{aligned}\sigma_{yy(j)}(\bar{x},\ \bar{y})&=-p_0\int_0^\infty\alpha T(\alpha)Q_{1j}(\alpha,\ \bar{y})\cos\alpha\bar{x}\,d\alpha\\ \sigma_{xy(j)}(\bar{x},\ \bar{y})&=ip_0\int_0^\infty\alpha T(\alpha)Q_{2j}(\alpha,\ \bar{y})\sin\alpha\bar{x}\,d\alpha\\ \sigma_{xx(j)}(\bar{x},\ \bar{y})&=p_0\int_0^\infty\alpha T(\alpha)Q_{3j}(\alpha,\ \bar{y})\cos\alpha\bar{x}\,d\alpha\end{aligned}\tag{20}$$

Here,

$$T(\alpha)=\int_0^1\sqrt{\tau}\,\Phi(\tau)J_0(\alpha\tau)d\tau\tag{21}$$

$$\begin{aligned}Q_{11}(\alpha,\ \bar{y})&=[F(\alpha)+\alpha\bar{y}b_1(\alpha)]\cosh\alpha\bar{y}+[c_1(\alpha)+\alpha\bar{y}d_1(\alpha)]\sinh\alpha\bar{y}\\ Q_{12}(\alpha,\ \bar{y})&=[F(\alpha)+\alpha\bar{y}b_1(\alpha)+d_1(\alpha)]\sinh\alpha\bar{y}+[b_1(\alpha)+c_1(\alpha)+\alpha\bar{y}d_1(\alpha)]\cosh\alpha\bar{y}\\ Q_{13}(\alpha,\ \bar{y})&=[F(\alpha)+\alpha\bar{y}b_1(\alpha)+2d_1(\alpha)]\cosh\alpha\bar{y}+[2b_1(\alpha)+c_1(\alpha)+\alpha\bar{y}d_1(\alpha)]\sinh\alpha\bar{y}\\ Q_{21}(\alpha,\ \bar{y})&=[a_0(\alpha)+\alpha\bar{y}b_0(\alpha)]e^{-\alpha\bar{y}}\\ Q_{22}(\alpha,\ \bar{y})&=[-a_0(\alpha)+(1-\alpha\bar{y})b_0(\alpha)]e^{-\alpha\bar{y}}\\ Q_{23}(\alpha,\ \bar{y})&=[a_0(\alpha)+(\alpha\bar{y}-2)b_0(\alpha)]e^{-\alpha\bar{y}}\end{aligned}\tag{22}$$

Numerical evaluation of the (20) can be made as follows,

$$\begin{aligned}\sigma_{yy(j)}(\bar{x},\ \bar{y})&=-p_0\sum_{h=0}^{N_h}\alpha_hT(\alpha_h)Q_{1j}(\alpha_h,\ \bar{y})\cos\alpha_h\bar{x}W(\alpha_h)\\ \sigma_{xy(j)}(\bar{x},\ \bar{y})&=ip_0\sum_{h=0}^{N_h}\alpha_hT(\alpha_h)Q_{2j}(\alpha_h,\ \bar{y})\sin\alpha_h\bar{x}W(\alpha_h)\\ \sigma_{xx(j)}(\bar{x},\ \bar{y})&=p_0\sum_{h=0}^{N_h}\alpha_hT(\alpha_h)Q_{3j}(\alpha_h,\ \bar{y})\cos\alpha_h\bar{x}W(\alpha_h)\end{aligned}\tag{23}$$

Here, N_h is the number of integration point with $W(\alpha_h)$ being the Simpson's weight factor.

2.4 Mises stress

The Mises stresses for the plane strain case, $\sigma_{eq(j)}$ for layer and substrate are as follows,

$$\sigma_{eq(j)}=\sqrt{\frac{1}{2}\{(\sigma_{1(j)}-\sigma_{2(j)})^2+(\sigma_{2(j)}-\sigma_{3(j)})^2+(\sigma_{3(j)}-\sigma_{1(j)})^2\}}\tag{24}$$

where,

$$\begin{aligned}\sigma_{1(j)}&=\frac{1}{2}(\sigma_{xx(j)}+\sigma_{yy(j)})+\sqrt{\sigma_{xy(j)}^2+\frac{1}{4}(\sigma_{xx(j)}-\sigma_{yy(j)})^2}\\ \sigma_{2(j)}&=\frac{1}{2}(\sigma_{xx(j)}+\sigma_{yy(j)})-\sqrt{\sigma_{xy(j)}^2+\frac{1}{4}(\sigma_{xx(j)}-\sigma_{yy(j)})^2}\\ \sigma_{3(j)}&=\nu_j(\sigma_{1(j)}+\sigma_{2(j)})\end{aligned}$$

2.5 Yield surface determination

Mises yield criterion for layer and substrate is as follows,

$$\sigma_{eq(1)}=\sigma_{y(1)},\quad\sigma_{eq(0)}=\sigma_{y(0)}\tag{25}$$

where, $\sigma_{y(1)}$ and $\sigma_{y(0)}$ are yield strengthes for layer and substrate, respectively.

Then, the yield surfaces for layer and substrate can be determined for given crack face pressure, p_0.

3. Numerical Results

Numerical analysis is performed for various layer-substrate combinations. The shear modulus ratio ($\Gamma=\mu_1/\mu_0$), crack length vs. layer thickness ratio(a/H), and Poisson's ratio(ν_j) are parameters for the analysis. First, the normal and shear stresses for the case of homogeneous material are calculated at several locations and showed good agreement with the results of Sneddon(Sneddon, 1946) as in Table. 1.

Table 1 Stress components comparison between sneddon(Sneddon, 1946) and current results for homogeneous case

		x=1.1 y=0.0	x=1.0 y=0.1	x=1.1 y=0.1	x=1.5 y=0.0	x=1.0 y=0.5	x=1.5 y=1.5
$\frac{\sigma_{yy(1)}}{p_0}$	Sneddon	1.4004	1.4299	1.5043	0.3416	0.1882	0.0491
	Current	1.4005	1.4299	1.5045	0.3416	0.1883	0.0491
$\frac{\sigma_{xx(1)}}{p_0}$	Sneddon	1.4004	-0.0257	0.3338	0.3416	-0.1996	-0.0848
	Current	1.4005	-0.0256	0.3338	0.3417	-0.1996	-0.0848
$\frac{\sigma_{xy(1)}}{p_0}$	Sneddon	0.0	-0.8460	0.1948	0.0	-0.4367	-0.1360
	Current	0.0	-0.8459	0.1949	0.0	-0.4367	-0.1360
$\frac{\sigma_{eq(1)}}{p_0}$	Sneddon	0.5602	1.9532	1.1299	0.1367	0.8275	0.2626
	Current	0.5602	1.9530	1.1301	0.1367	0.8276	0.2626

Figure 2 is the normal stresses in y direction at the mid-plane for various shear modulus ratios and crack length vs. layer thickness ratios. The stress is most concentrated near crack tip for thin stiff layer case (a/H=4.0, Γ=4.0). Figure 3 is the normal and shear interfacial stresses between the layer and the substrate. It is noted that normal stress in x direction is discontinuous at the layer-substrate interface due to the material mis-match. The maximum mis-match occurred above the crack location for thin stiff layer case(a/H=4.0, Γ=4.0).

Figure 4 is the normal stress contours and Fig. 5 is the shear stress contours for various layer-substrate combinations. The maximum contour level is 1.3 p_0 with each contour interval being 0.1 p_0. When the layer is thin(a/H=4.0), the stress distributions are influenced by the shear modulus ratios; For stiff layer case(Γ=4.0), the resultant

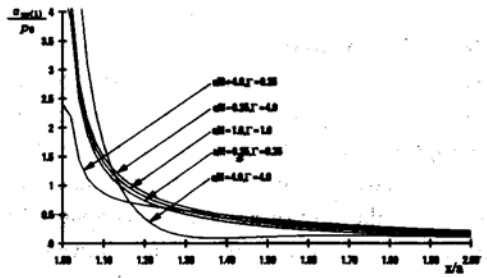

Fig. 2 Normal stress distributions at mid-plane for various Γ and a/H

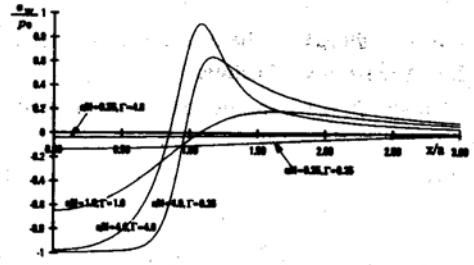

(a) σ_{yy}/p_0

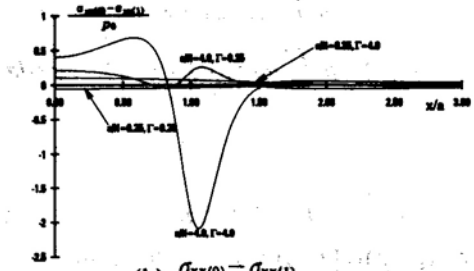

(b) $\frac{\sigma_{xx(0)} - \sigma_{xx(1)}}{p_0}$

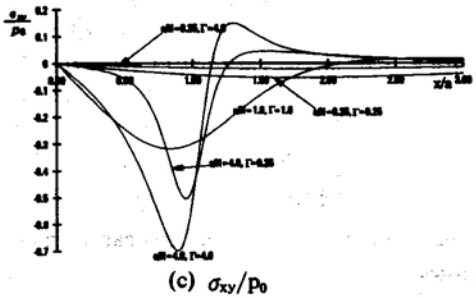

(c) σ_{xy}/p_0

Fig. 3 Interfacial stress distribution for various Γ and a/H

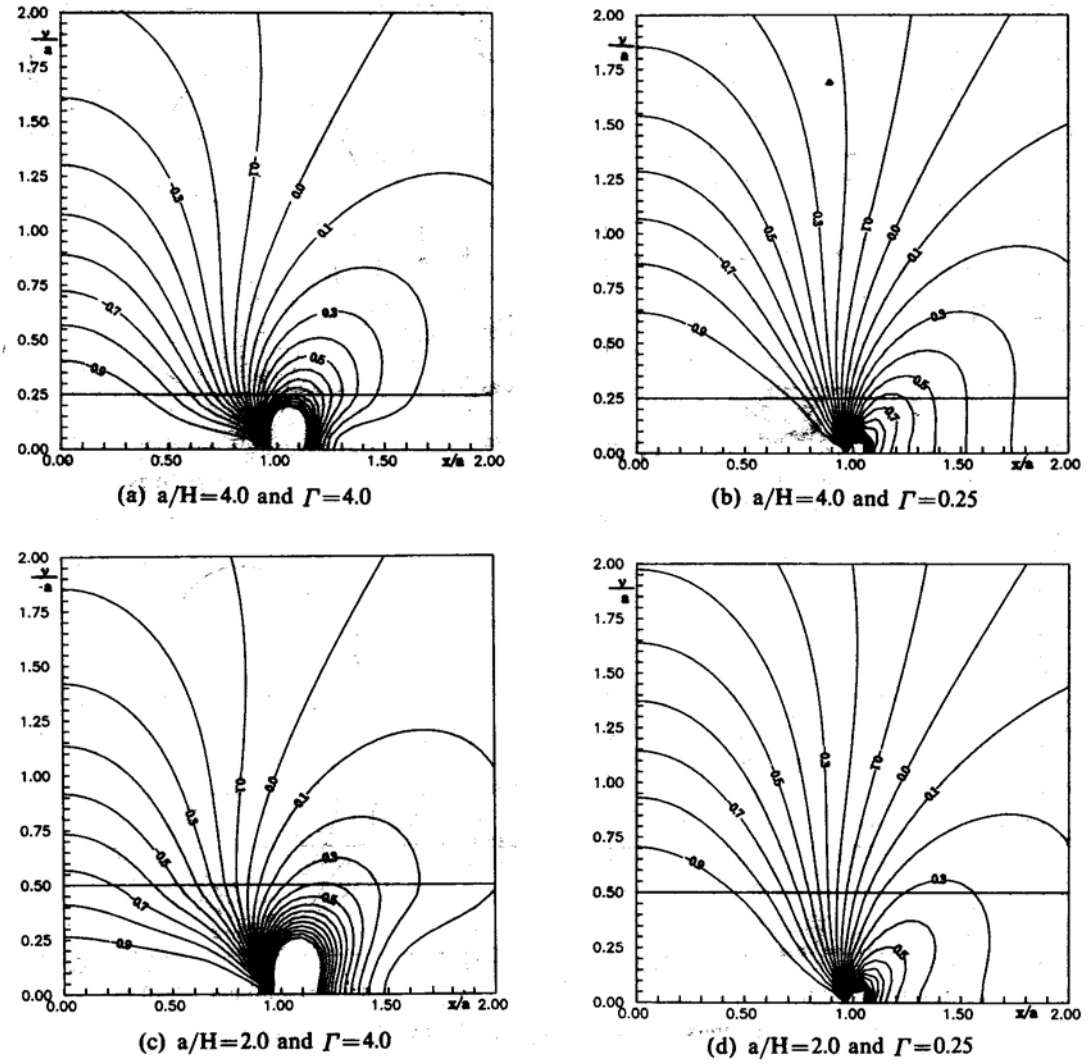

(a) a/H=4.0 and Γ=4.0 (b) a/H=4.0 and Γ=0.25

(c) a/H=2.0 and Γ=4.0 (d) a/H=2.0 and Γ=0.25

Fig. 4 Normal stress contours for various Γ and a/H ($\sigma_{yy(1)}/p_0$)

stresses in the layer are higher than those of soft layer case(Γ=0.25) while the substrate stress is slightly lower than that of soft layer case(Γ=0.25). When the layer is relatively thick(a/H=1.0), however, the stress distributions are nearly influenced by the shear modulus ratios because in that case the inhomogeneity between the layer and the substrate is remotely localized and therefore does not influence the stress fields as stated in the Saint-Venant's principle.

Similar results are obtained on the Mises stress contour as shown in Fig. 6. It is also noted that the Mises stress is discontinuous at the layer-substrate interface due to the material mis-match. Figure 7 is the yield surface deterimined from the Mises yield criterion for various crack surface pressure p_0. Two cases of layer-substrate combinations are considered ; The tungsten layer bonded to steel substrate and copper layer bonded to steel substrate represent the case of hard layer and the case of soft layer, respectively with the material properties as in Table. 2. When the crack surface pressure is 300MPa, the hard layer case resulted in smaller yield region confined in the layer

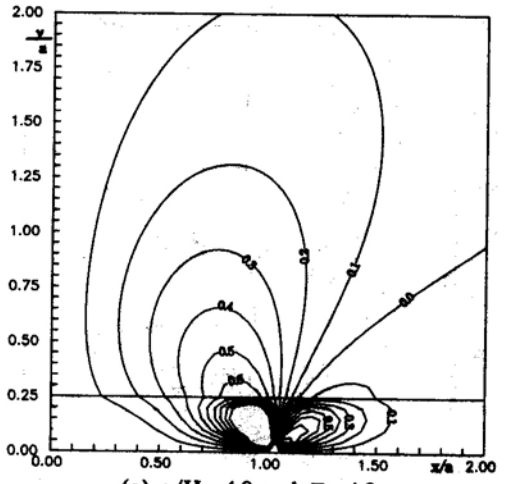

(a) a/H=4.0 and Γ=4.0

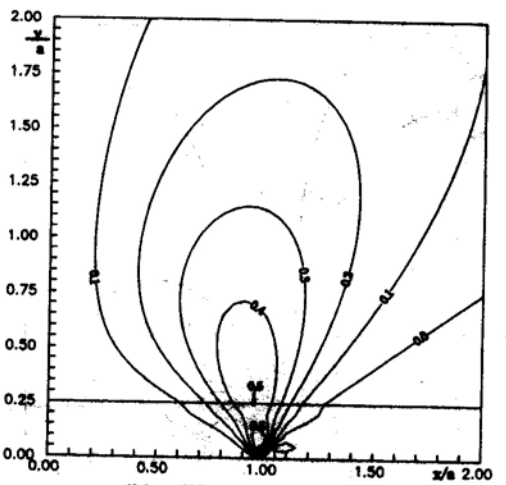

(b) a/H=4.0 and Γ=0.25

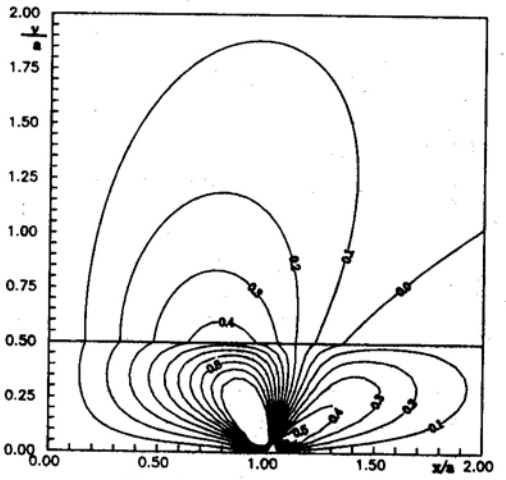

(c) a/H=2.0 and Γ=4.0

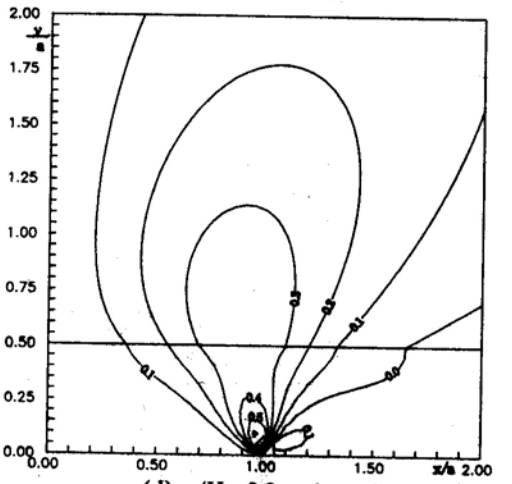

(d) a/H=2.0 and Γ=0.25

Fig. 5 Shear stress contours for various Γ and a/H ($\sigma_{xy(i)}/p_0$)

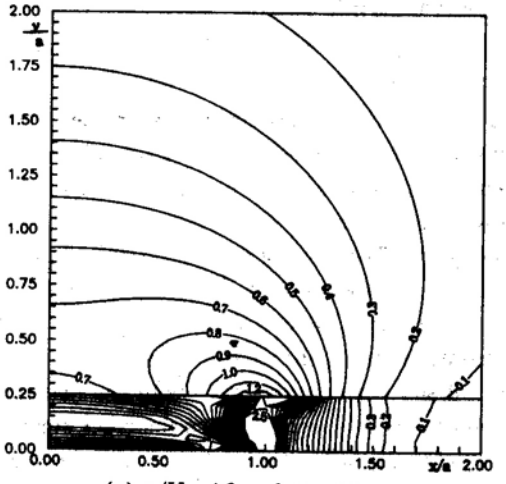

(a) a/H=4.0 and Γ=4.0

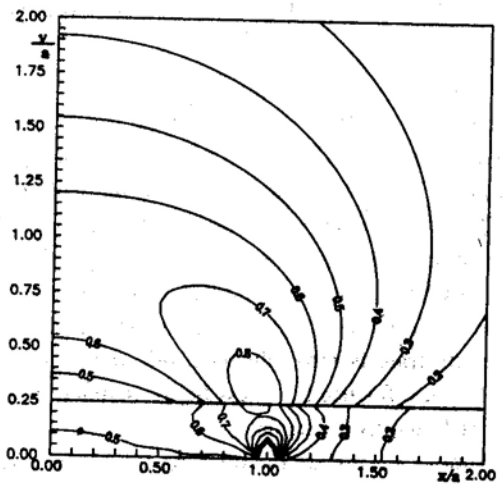

(b) a/H=4.0 and Γ=0.25

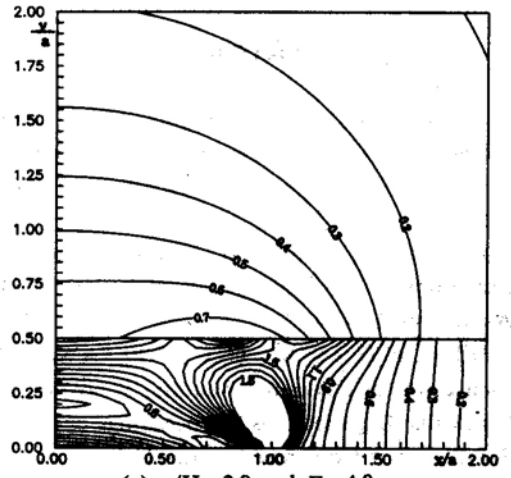

(c) a/H=2.0 and Γ=4.0

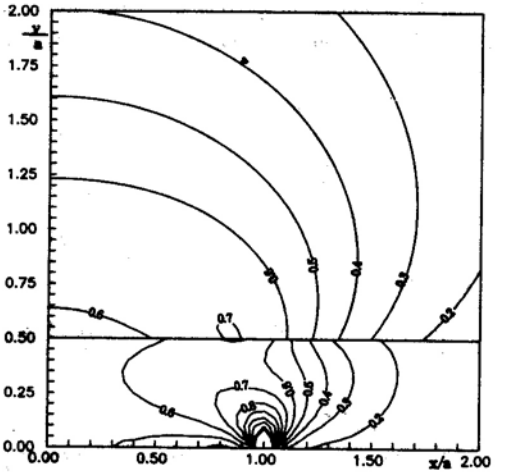

(d) a/H=2.0 and Γ=0.25

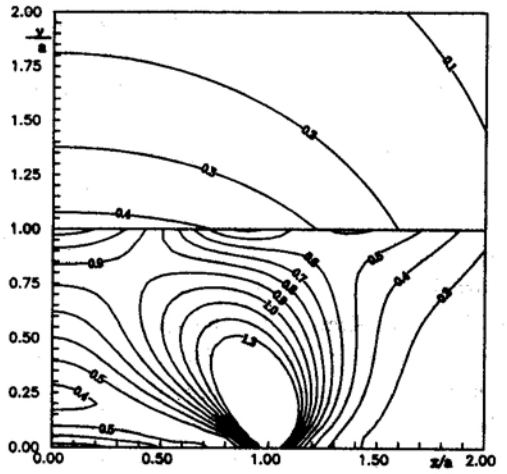

(e) a/H=1.0 and Γ=4.0

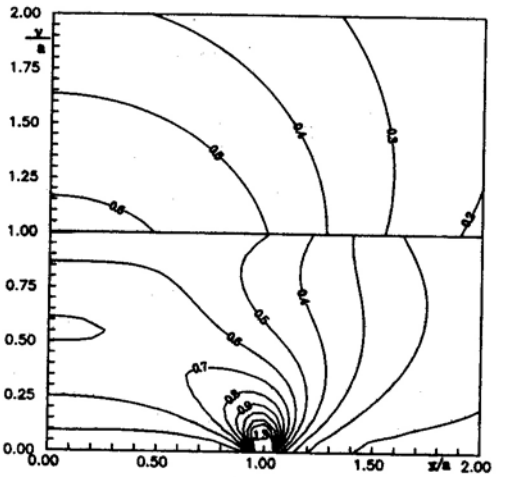

(f) a/H=1.0 and Γ=0.25

Fig. 6 Mises stress contours for various Γ and a/H ($\sigma_{eq(J)}/p_0$)

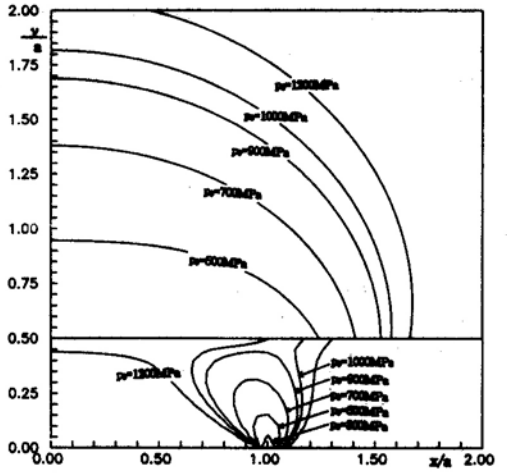

Fig. 7 Yield surface for hard layer case (tungsten layer bonded to steel substrate)

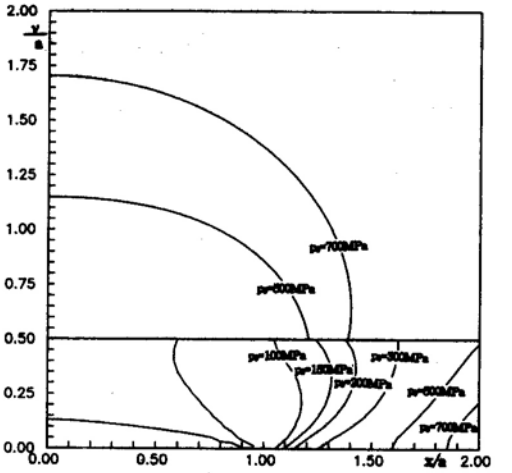

Fig. 8 Yield surface for soft layer case (copper layer bonded to steel substrate)

Table. 2 Material properties for hard layer case (tungsten layer bonded to steel substrate) and soft layer case(copper layer bonded to steel substrate)

	Shear modulus (μ)	Yield strength (σ_Y)
Steel	80 GPa	300 MPa
Tungsten	160 GPa	1,000 MPa
Copper	45 GPa	70 MPa

whereas the soft layer case resulted in larger yield region extended to the layer-substrate interface.

4. Conclusions

The stress distributions and yield surface for cracked layer perfectly bonded to the substrate are analyzed. By following the theory of linear elasticity, a Fredholm integral equation is derived in matrix form which may enable the future analysis for multiple layer case, and solved numerically. The stress components as well as the Mises stresses are evaluated for various layer-substrate combinations. When the layer is thin, the stress distributions are clearly influenced by the shear modulus ratios between the layer and the substrate. Finally, using the Mises yield criterion, the yield region is determined for hard layer case and soft layer case. The hard layer case resulted in smaller yield region confined in the layer whereas the soft layer case resulted in larger yield region extended to the layer-substrate interface.

References

Abramowitz, M. and Stegun, I. A., 1970, *Handbook of Mathematical Functions(with Formulas, Graphs and Mathematical Tables)*, Dover.

Copson, E. T., 1961, "On Certain Dual Integral Equations," Proceedings of Glasgow Math. Assoc., pp. 19~24.

Hilton, P. D. and Sih, G. C., 1970, "A Sandwiched Layer of Dissimilar Material Weakened by Crack-like Imperfections," Proceedings of the 5th South-eastern Conference on the Theoretical and Applied Mechanics, Vol. 5, pp. 123~149.

Hilton, P. D. and Sih, G. C., 1971, "A Laminated Composite with a Crack Normal to the Interface," International Journal of Solids and Structures, Vol. 7, pp. 913~930.

Kim, S. H., Oh, J. H. and Ong, J. W., 1991, "Stress Intensity Factors for Center Cracked Laminated Composites under Uniaxial Tension," The Korean Society of Mechanical Engineers, Journal, Vol. 15, No. 5, pp. 1611~1619.

Oh, J. H., Kim, S. H. and Ong, J. W., 1992, "Stress Intensity Factors for Center Cracked Laminated Composites under Shear Loading," The Korean Society of Mechanical Engineers, Journal, Vol. 16, No. 5, pp. 838~848.

Sneddon, I. N., 1946, "The Distribution of Stress in the Neighbourhood of a Crack in an Elastic Solid," Proceedings of Royal Society of London, Vol. 187, pp. 229~260.

Sneddon, I. N., 1951, *Fourier Transforms*, McGraw Hill.